

Relation between winding numbers and energy dispersions

Quancheng Liu¹ and Klaus Ziegler^{2,3}

¹School of Physics, State Key Laboratory of Crystal Materials,
Shandong University, Jinan 250100, China

²Institut für Physik, Universität Augsburg, D-86135 Augsburg, Germany

³Physics Department, New York City College of Technology,
The City University of New York, Brooklyn, NY 11201, USA

(Dated: December 30, 2025)

Abstract:

Two-band Hamiltonians provide a typical description of topological band structures, in which the eigenfunctions can be characterized by a winding number that defines an integer topological invariant. This winding number is quantized and protected against continuous deformations of the Hamiltonian. Here we show that the Bloch vector and its winding number can be directly related to the gradient of the energy dispersion. Since the energy gradient is proportional to the group velocity, our result establishes an experimentally accessible correspondence between the Bloch vector field and angle-resolved photoemission spectroscopy measurements. We discuss a mapping between the gradient of the energy dispersion and the Bloch vector. This implies a direct and measurable relation between two-band Hamiltonians and their underlying topological structures.

In two-dimensional materials topological properties can play a crucial role. Their discovery was very successful in explaining the quantum Hall effect [1], since the Hall conductivity is a topological invariant [2–5]. Topological properties are also essential for the quantum spin Hall effect [6–9]. More recent works on artificial materials (e.g., Floquet dynamics on systems of quantum wells and waveguides) have focused on various topological properties [10–13]. This is often motivated by the existence of topological invariants such as the Berry phase or Chern numbers. In contrast to the quantum Hall effect, in these systems the topological invariants are not always directly accessible and are more difficult to detect [12] or to calculate [11, 14, 15]. Therefore, it might be also of practical interest to probe topological properties with tomographic methods. In the following we propose to extend the study of invariants to the analysis of trajectories on the Bloch sphere and their winding numbers. Our quantum systems are described by a Hamiltonian of the simple form $\vec{\chi} \cdot \vec{\sigma}$ with the vector of Pauli matrices $\vec{\sigma}$, introduced for the quantum Hall effect without Landau levels [3] and discussed subsequently in numerous papers [4, 16–18].

In a typical study only the eigenfunctions, but not the eigenvalues, reflect the topological properties of a Hamiltonian [4, 16, 17, 19, 20], such as the winding number of the eigenfunctions or the Berry phase. In this Letter we will argue that also the eigenvalues of a translation-invariant Hamiltonian can be used to calculate the winding number. This offers an approach to probe topological properties within conventional experimental techniques, such as Angle-Resolved Photoemission Spectroscopy (ARPES). For this purpose we consider a translation-invariant Hamiltonian on a physical space where the latter is either two dimensional with real coordinates \mathbf{r} or a corresponding Fourier space with wave vector \mathbf{k} . Edges can be added subsequently and treated either through the topological bulk-edge correspondence [21, 22] or through the analytic bulk-edge connection (ABEC) [23]. Moreover, we assume that H acts on a two-component spinor space (“two-band model”), such that its eigenfunctions $\{\Psi_k\}$ are two-component spinors.

The main idea is based on an intimate connection between the energy eigenvalues and the Bloch vector (BV), which can be seen in the change of the eigenvalue $E_k = (\Psi_k \cdot H \Psi_k)$ under the change of the Hamiltonian H . Ψ_k is the normalized eigenfunction $\Psi_k(\mathbf{r})$ and the brackets represent the spatial integration, where \mathbf{r} are the coordinates on the physical space. In the case of translation invariance the eigenfunctions are plane waves or in the case of rotational invariance they are spherical waves. The latter is applicable to a circular disk-like geometry [24, 25], but this case will not be pursued subsequently. In general, an infinitesimal change of E_k with respect to a parameter x reads

$$\partial_x E_k = (\Psi_k \cdot (\partial_x H) \Psi_k), \quad (1)$$

since $(\Psi_k \cdot H(\partial_x \Psi_k)) + ((\partial_x \Psi_k) \cdot H \Psi_k) = E_k \partial_x (\Psi_k \cdot \Psi_k) = 0$ due to $(\Psi_k \cdot \Psi_k) = 1$. For the operator-valued Hamiltonian $H = \vec{\chi} \cdot \vec{\sigma}$, we assume that $\vec{\chi} \Psi_k = \vec{h} \Psi_k$ with a number-valued vector $\vec{h}(\mathbf{k})$ [3, 4, 16], where

the specific choice of the eigenfunctions ψ_k is dictated by geometry. Then a simple relation between energy eigenvalues and the components of the BV $\vec{s}_k = (\Psi_k \cdot \vec{\sigma} \Psi_k)$ emerges as

$$\nabla_{\vec{h}} E_k = \vec{s}_k. \quad (2)$$

On the other hand, the eigenvalues of the 2×2 matrix $H = \vec{h} \cdot \vec{\sigma}$ are $E_k = \pm h$, such that Eq. (2) implies for the BV

$$\vec{s}_k = \pm \frac{1}{h} \vec{h}. \quad (3)$$

Thus, the BV field \vec{s}_k is the result of a map from the physical space to the Bloch sphere S^2 . In particular, a closed trajectory in the physical space results in a closed trajectory on the Bloch sphere, which is either a single point, an open line, a single loop or a multiple loop with an integer winding number more than 1 or less than -1. Hence the winding numbers yield a classification of different maps $\vec{h} \rightarrow \vec{s}_k$. Moreover, relation (3), which we derived from Eqs. (1) and (2), enables us to recover the normalized vector \vec{h} of the Hamiltonian from \vec{s}_k , while relation (2) recovers the gradient of the energy dispersion from \vec{s}_k . In other words, for a given \vec{h} we obtain directly the BV field from these relations, without an explicit calculation of its eigenfunctions. Thus, the mapping provides important information such as the topologically protected winding number.

Examples: To illustrate the usefulness of the relations (2) and (3) in terms of a winding-number classification we consider some examples. The first example is a two-band Laplacian Hamiltonian with mass m and $\vec{h}(k) = (k^2, 0, m)^T$, which represents a semi-conducting system with time-reversal symmetry. Its eigenvalue reads $E_k = \pm \sqrt{k^4 + m^2}$ and its BV has only North-South trajectories. Thus, it has the winding number $n_w = 0$. The second example is the 2D Dirac Hamiltonian in Fourier space with $\vec{h}(\mathbf{k}) = (k_x, k_y, m)^T$ and energy dispersion $E_k = \pm \sqrt{k^2 + m^2}$. Replacing the Dirac mass m by a third component of the wave vector k_z we obtain the 3D Weyl Hamiltonian [26, 27], where the BV of the former is the map $T^2 \rightarrow S^2$ and the BV of the latter $T^3 \rightarrow S^2$. These Hamiltonians have a winding number $n_w = 1$.

A related lattice version of the 2D Dirac Hamiltonian is the tight-binding Hamiltonian on the honeycomb lattice with

$$\vec{h}(\mathbf{k}) = (d', d'', m)^T, \quad d' = \sum_{\mu} \cos(\mathbf{a}_{\mu} \cdot \mathbf{k}), \quad d'' = \sum_{\mu} \sin(\mathbf{a}_{\mu} \cdot \mathbf{k}) \quad (4)$$

with $\mathbf{a}_1 = a(0, -1)$ and $\mathbf{a}_{2,3} = a(\pm\sqrt{3}, 1)/2$ for a lattice constant a . This Hamiltonian is time-reversal invariant, in contrast to the 2D Dirac or 3D Weyl Hamiltonians. In the lattice case the trajectory of the BV of a circle in \mathbf{k} space is more complex. In particular, its winding number is not robust for all trajectories and, therefore, cannot be associated with an invariant, as visualized in Fig.1a): it is ± 1 only near the nodes. This property is often used to obtain an integer Hall conductivity in low-energy approximation [3, 17], where only small deviations from the nodes are considered. However, the integral over the entire Brillouin zone (i.e. the Chern number) vanishes here due to the time-reversal invariance, as for the two-band Laplacian Hamiltonian. Nevertheless, the trajectories on the Bloch sphere are quite different for both models, reflecting different topological properties. All these Hamiltonians have been discussed extensively in the existing literature, especially in the low-energy projection [3, 4, 16–18].

The third example for $\vec{h} \cdot \vec{\sigma}$ is the Bogoliubov de Gennes (BdG) Hamiltonian that is qualitatively different, since, in contrast to the other examples, the BV field is now hosted in a four-dimensional space with coordinates \mathbf{k} and \mathbf{r} such that the BV is the result of the mapping $T^2 \times T^2 \rightarrow S^2$. A non-uniform order parameter $\Delta(\mathbf{r}) = \Delta'(\mathbf{r}) + i\Delta''(\mathbf{r})$ describes the Josephson effect [28] and \vec{h} is defined as

$$\vec{h}(\mathbf{r}, \mathbf{k}) = (\Delta'(\mathbf{r}), \Delta''(\mathbf{r}), h_3(\mathbf{k}))^T \quad (5)$$

with energy dispersion $E_k = \pm \sqrt{|\Delta|^2 + h_3(\mathbf{k})}$. The order parameter reduces the translation invariance of the operator χ_3 . For example, if it is periodic on the torus of length L in x direction with periodicity w , i.e., $\Delta = |\Delta| \exp(2\pi i w x / L)$, the winding number of the BV is $n_w = w$. Thus, we can control the winding by the choice of the periodic order parameter and create a sequence of topological transitions [29]. Parametrizing a trajectory on $T^2 \times T^2$ as $h_3 = 2 + \cos^2 t$ and $x = t$ for $0 \leq t < 2\pi$, with $w = 3$ the trajectory on the Bloch sphere has winding number $n_w = 3$, as visualized in Fig. 1b).

Physical interpretation of the BV: It is well known that \vec{h}/\hbar of the Hamiltonian $\vec{h} \cdot \vec{\sigma}$ is directly linked to the Berry curvature [4, 17, 18]. This can be used to obtain the topological charge (or Chern number) as the integral over the Brillouin zone (BZ)

$$C_{\pm} = \pm \frac{1}{4\pi} \int_{\text{BZ}} \vec{s} \cdot (\partial_{k_x} \vec{s} \times \partial_{k_y} \vec{s}) d^2 \mathbf{k}, \quad (6)$$

which has been linked to the Hall conductivity [4, 16]. With Eq. (2) we can relate C_{\pm} to the gradient of the energy dispersion now. The BV field provides more information than this integral though. In particular, while the integral vanishes or gives an integer, the BV field provides specific trajectories on the Bloch sphere in subspaces of the BZ, which characterize local properties, for instance, a winding number near spectral nodes. Thus, it is suited for a tomographic analysis of complex quantum systems.

Since the BV field is a gradient field with respect to \vec{h} , it is free of vortices. However, it also depends on the physical space coordinates, either in real or Fourier space. For instance, experimentally we may observe the dispersion as a function of the wave vector \mathbf{k} . To study the group velocity $\hbar \mathbf{v}_k = \nabla_{\mathbf{k}} E_k$ in ARPES [19], we may consider the gradient of the dispersion as

$$\nabla_{\mathbf{k}} E_k = \sum_{\nu} \frac{\partial E_k}{\partial h_{\nu}} \nabla_{\mathbf{k}} h_{\nu} = \vec{s}_k \cdot \nabla_{\mathbf{k}} \vec{h}, \quad (7)$$

while a direct calculation yields $\nabla_{\mathbf{k}} E_k = \pm \nabla_{\mathbf{k}} h$ due to $E_k = \pm h$. For the 2D Dirac and 3D Weyl Hamiltonian, where we have a linear dispersion, the gradient of the dispersion reproduces the BV field. In contrast, the BdG Hamiltonian leads to a gradient of the dispersion whose third component does not agree to the third component of the BV.

Besides the gradient of the energy dispersion in Eq. (2), another interesting analysis of the BV is associated with expectation values of the spinor components. This can be understood when we define for two spinor components ψ_1 and ψ_2 of $\Psi_k = (\psi_1, \psi_2)^T$ the following wave functions

$$\psi_{\pm} := \psi_1 \pm \psi_2, \quad \psi'_{\pm} := \psi_1 \pm i\psi_2 \quad (8)$$

and the corresponding probabilities $P_j = (\psi_j \cdot \Psi_j)$ as well as

$$P_{\pm} := (\psi_{\pm} \cdot \psi_{\pm}), \quad P'_{\pm} := (\psi'_{\pm} \cdot \psi'_{\pm}). \quad (9)$$

Then a straightforward calculation yields

$$\vec{s}_k = \begin{pmatrix} P_+ - P_- \\ P'_- - P'_+ \\ P_1 - P_2 \end{pmatrix}, \quad (10)$$

where the third component describes the polarization $2P_1 - 1$ of the two bands, since $P_1 + P_2 = 1$. The other two components represent the polarization of the super-positioned wave functions in Eq. (8). This form of \vec{s}_k is also known as the Stokes vector in classical optics and light scattering [30, 31]. To measure these probabilities we must have access to both spinor components individually, which might be possible with Spin-ARPES [32, 33].

Edge modes: So far, our discussion has focused on a compact physical space without edges, as presented by a torus. For an additional edge, obtained by drilling a hole or cutting the torus, the properties of the edge modes can be derived via the ABEC through an analytic continuation $k_j \rightarrow ic_j$ under the condition that the eigenvalues are real [23]. We note that this approach is based on the eigenfunctions in contrast to the topological bulk-edge correspondence [21, 22], which is based on the relation of the topological indices of the bulk (typically the Chern numbers) and the number of edge states. The analytic continuation results in a BV field, in which an imaginary wave number represents a bound state in the direction perpendicular to the edge. The ABEC has some similarity with the concept of the Generalized Brillouin Zone (GBZ) for non-Hermitian systems. In the latter, the eigenvalues are imaginary though [34], while in the ABEC all eigenvalues are real.

For the BdG Hamiltonian, an edge along the x -axis creates edge modes in the y -direction and a BV field $\vec{s}_k(\mathbf{r}, k_x, ic_y)$ with real k_x and c_y . Boundary conditions on the edge fixes c_y but leave \mathbf{r} and k_x as quasi-continuous variables. Thus, the BV can be parametrized by the three-dimensional x - y - k_x coordinates, where loops in this space create winding trajectories on the Bloch sphere as those visualized in Fig. 1b).

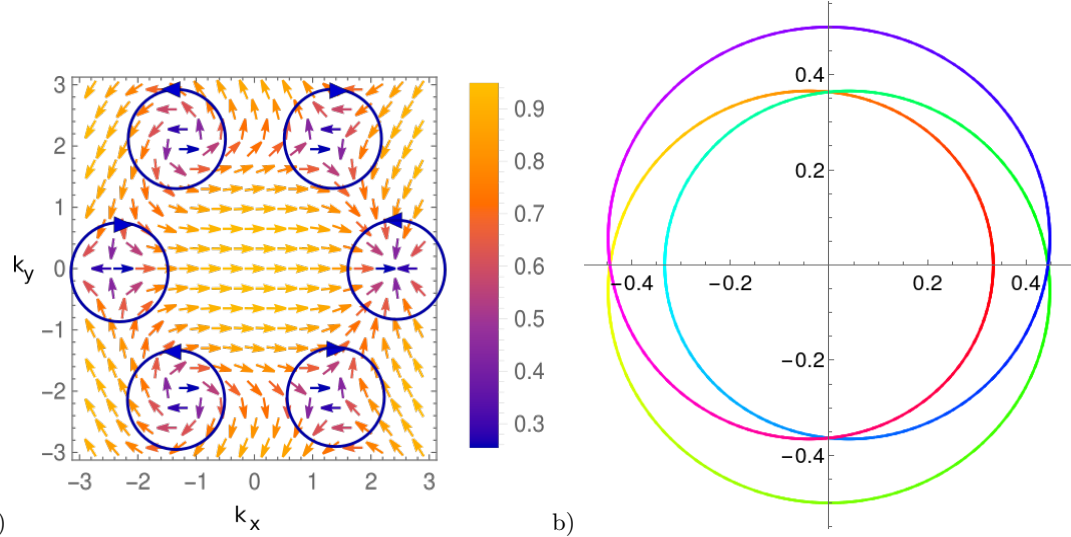


FIG. 1. 2D projection of the BV field: a) The BV field of a tight-binding Hamiltonian on a honeycomb lattice has several nodes. The marked loops around these nodes have the winding numbers ± 1 , indicated by the clockwise or counter-clockwise winding, respectively. The actual length of the s_1-s_2 projected BV is color encoded. b) The winding trajectory of the BV of the BdG Hamiltonian with $w = n_w = 3$. The continuous color change indicates the evolution of the trajectory with t for $0 \leq t < 2\pi$.

Conclusions: We have derived a direct relation between the $SU(2)$ Hamiltonian $\vec{\chi} \cdot \vec{\sigma}$ and the associated BV field, as given in Eq. (3). A central result is that the BV can be obtained directly from the gradient of the energy dispersion Eq. (2), such that the band structure alone suffices to reconstruct the BV. While the BV yields the Chern number via Eq. (6), it provides a more general characterization that does not rely on integration over a predefined region of momentum space, allowing for flexible boundary conditions and local topological analysis. Our approach establishes a direct identification between the BV, the energy dispersion, and the vector \vec{h} of the $SU(2)$ Hamiltonian. Experimentally, the relation between the BV and the energy gradient implies that angle-resolved photoemission spectroscopy can access the BV field through measurements of the group velocity Eq. (7). Finally, we have seen that Hamiltonians of the form $\vec{\chi} \cdot \vec{\sigma}$ can be classified by the winding numbers of the BV field, providing a topological characterization based on invariant subspaces rather than global integrals.

[1] K. v. Klitzing, G. Dorda and M. Pepper. *New method for high-accuracy determination of the fine-structure constant based on quantized hall resistance*, Phys. Rev. Lett. 45, 494–497 (1980).

[2] D.J. Thouless, M. Kohmoto, M.P. Nightingale, and M. den Nijs. *Quantized Hall Conductance in a Two-Dimensional Periodic Potential*, Phys. Rev. Lett 49, 405 (1982).

[3] F.D.M. Haldane. *Model for a Quantum Hall Effect without Landau Levels: Condensed-Matter Realization of the "Parity Anomaly"*, Phys. Rev. Lett. 61, 2015 (1988).

[4] V.M. Yakovenko. *Chern-Simons Terms and n Field in Haldane's Model for the Quantum Hall Effect without Landau Levels*, Phys. Rev. Lett. 65, 251 (1990).

[5] Y. Hatsugai. *Chern number and edge states in the integer quantum Hall effect*, Phys. Rev. Lett. 71, 3697 (1993).

[6] C. L. Kane and E.J. Mele. *Z_2 topological order and the quantum spin hall effect*, Phys. Rev. Lett. 95, 146802 (2005).

[7] C.L. Kane and E.J. Mele. *Quantum spin hall effect in graphene*, Phys. Rev. Lett. 95, 226801 (2005).

[8] B. A. Bernevig and S. C. Zhang. *Quantum spin hall effect*, Phys. Rev. Lett. 96, 106802 (2006).

[9] M. König, S. Wiedmann, C. Brüne, A. Roth, H. Buhmann, L.W. Molenkamp, X.-L. Qi, S.-C. Zhang, *Quantum spin hall insulator state in HgTe quantum wells*, Science 318, 766–770 (2007).

[10] N.H. Lindner, G. Refael and V. Galitski. *Floquet topological insulator in semiconductor quantum wells*, Nature Phys. 7, 490 (2011).

- [11] M.S. Rudner, N.H. Lindner, E. Berg, and M. Levin. *Anomalous Edge States and the Bulk-Edge Correspondence for Periodically Driven Two-Dimensional Systems*, Phys. Rev. X 3, 031005 (2013).
- [12] M.C. Rechtsman, J.M. Zeuner, Y. Plotnik, Y. Lumer, D. Podolsky, F. Dreisow, S. Nolte, M. Segev, and A. Szameit. *Photonic Floquet topological insulators*, Nature 496, 196 (2013).
- [13] Q. Liu, W. Liu, Y. Jia, K. Ziegler, A. Alù, F. Chen. *Measurement-induced photonic topological insulators*, Sci. Adv. 11, eadx0595 (2025).
- [14] T. Fukui, Y. Hatsugai and H. Suzuki. *Chern Numbers in Discretized Brillouin Zone: Efficient Method of Computing (Spin) Hall Conductances*, Journ. Phys. Soc. Jap. 74, 1674 (2005).
- [15] B. Höckendorf, A. Alvermann and H. Fehske. *Efficient computation of the W3 topological invariant and application to Floquet-Bloch systems*, J. Phys. A: Math. Theor. 50, 295301 (2017).
- [16] X.-L. Qi, Y.-S. Wu, and S.-C. Zhang. *Topological quantization of the spin Hall effect in two-dimensional paramagnetic semiconductors*, Phys. Rev. B74, 085308 (2006).
- [17] E. Fradkin. *Field Theories of Condensed Matter Physics*, Cambridge University Press (2013).
- [18] J.E. Moore, Y. Ran and X.-G. Wen. *Topological surface states in three-dimensional magnetic insulators*, Phys. Rev. Lett. 101, 186805 (2008).
- [19] J. Moore. *The birth of topological insulators*, Nature 464, 194–198 (2010).
- [20] B. Keimer and J. Moore. *The physics of quantum materials*, Nature Phys 13, 1045–1055 (2017).
- [21] G.M. Graf and M. Porta. *Bulk-edge correspondence for two-dimensional topological insulators*, Comm. Math. Phys., 324(3):851–895 (2013).
- [22] J. Shapiro. *The bulk-edge correspondence in three simple cases*, Reviews in Mathematical Physics 32 (03), 2030003 (2020).
- [23] K. Ziegler. *Analytic bulk-edge connection in circular-symmetric models*, J. Phys. A: Math. Theor. 58 345301 (2025).
- [24] K. Ziegler. *Circular edge states in photonic crystals with a dirac node* J. Opt. Soc. Am. B 35, 107 (2018).
- [25] K. Ziegler and R.Ya. Kezerashvili. *Edge modes in chiral electron double layers*, Phys. Rev. B, 111:L140507 (2025).
- [26] N.P. Armitage, E.J. Mele and A. Vishwanath. *Weyl and Dirac semimetals in three-dimensional solids*, Rev. Mod. Phys. 90, 015001 (2018).
- [27] A.A. Burkov. *Weyl metals*, Annual Review of Condensed Matter Physics Volume 9, (2018).
- [28] B. Josephson. *Possible new effects in superconductive tunnelling*, Physics Letters 1, 251 (1962).
- [29] K. Ziegler. *Josephson effect with periodic order parameter*, arXiv:2510.26128.
- [30] H.C. van de Hulst. *Light Scattering by Small Particles*, Dover Publications (New York 1981).
- [31] M. I. Mishchenko, L. D. Travis and A. A. Lacis. *Multiple scattering of light by particles* Cambridge University Press (2006).
- [32] S. LaShell, B.A. McDougall, and E. Jensen. *Spin Splitting of an Au(111) Surface State Band Observed with Angle Resolved Photoelectron Spectroscopy*, Phys. Rev. Lett. 77, 3419 (1996).
- [33] J. Hu, D. W. Shen and D.L. Feng. *Spin polarization and dichroism effects induced by an electric field*, Phys. Rev. B 73, 085325 (2006).
- [34] K. Yokomizo and S. Murakami. *Non-Bloch band theory in bosonic Bogoliubov-de Gennes systems*, Phys. Rev. B103,165123 (2021).